International Journal of Technology 14(3) 536-548 (2023)
Received October 2022 / Revised November 2022 / Accepted December 2022

International Journal of Technology

http://ijtech.eng.ui.ac.id

Traction Force Investigation of The New Working Body of The Sod Seeder

Sayakhat Nukeshev[1*], Kairat Yeskhozhin[1], Yerzhan Akhmetov[1], Dinara Kossatbekova[1], Kaldibek Tleumbetov[1], Khozhakeldi Tanbayev[1]

[1]*Department of Technical Mechanics, NCJSC S. Seifullin Kazakh AgroTechnical Research University, Zhenis avenue 62, 010011 Astana, Kazakhstan*

Abstract. Due to the depletion of pastures, fodder provisioning is becoming an acute problem, therefore improving pastures by sowing seeds undercover crops and in turf is essential. The main purpose of the work is to reduce the traction force of the sod seeder by developing an effective working body. As a result, a new technology for improving forage and pasture lands and the design of a working body of sod seeder for site-specific seeding of crops undercover crops are proposed. The new technology provides simultaneous sowing of grass seed and fertilizer at two levels of soil horizon without excluding the forage area from the exploitation: grass seed to a depth of 40 mm and fertilizer to a depth of 120 mm. The seed sowing and fertilizer application depths are adjustable, and the sowing width reaches 40 mm. The traction force was determined by the dynamometric method during laboratory and field experiments. Theoretical studies have determined the dependence of the traction force on the average parameters of the cultivated soil layer and its physical and mechanical properties, as well as the parameters of the working body. According to the results of experimental and field studies, the traction force range of the sod seeder was within 8.28–8.63 kN.

Keywords: Cover crops; Hoe opener; Meadow and pasture restoration; Mineral fertilizers; Site-specific seeding; Traction force

1. Introduction

Arid pastures are a major source of forage for cattle and sheep in many countries. In turn, high-yielding forage grass species are essential components of sustainable pasture production and provide valuable ecosystem services (Adams *et al.*, 2022; Karimipoor *et al.*, 2021). Therefore, it is necessary to improve pastures by sowing seeds under cover crops and on turf (Himmelbauer *et al.*, 2013; Bathgate, Revell, and Kingwell, 2009). Currently, the radical improvement of pastures, including a full range of operations to create a new grass shank by sowing seeds of perennial grasses requires significant financial costs and is carried out very rarely (Fulkerson and Lowe, 2022; Soldatov *et al.*, 2020; Zotov *et al.*, 2012). The majority of technologies for restoring the biological productivity of natural grasslands are based on scattered grass seeding or direct seeding, which involves cutting furrows in the turf and seeding grass seeds. Scattered seeding is not sufficiently effective on neglected grasslands, and the use of herbicides significantly increases the cost of technology and environmental safety requirements (Scotton, 2019; Deák *et al.*, 2018; Benincasa

*Corresponding author's email: s.nukeshev@kazatu.kz, Tel.: +7-7015129791; Fax: +7 (7172) 31-60-72
doi: 10.14716/ijtech.v14i3.6008

et al., 2017). In addition, the conditions of uncultivated, unprepared land with roots of old-age grasses make the sowing work difficult. The quality of grass seed sowing with sod seeding machines mostly depends on the colter's performance, which ensures the formation of optimal conditions for seed germination and further plant development. A hoe opener, for example, has been designed considering the optimal parameters of the mechanically cut strip in turf for each zone. However, during the operation of seeders, it is necessary to quickly adapt the tillage part to changing working conditions, such as the degree of sodding, physical and mechanical soil parameters, etc. In this case, the adjustment of seeders to changing conditions of operation can be rationally carried out by replacing the working bodies (Sysuev *et al.*, 2022; Revenko and Belousov, 2014; Bowman *et al.*, 2008). In turn, it requires new research on the development, and the study of a new design of the hoe opener is required as well.

A promising alternative is to sow grass into a strip of mechanically destroyed turf without excluding the forage area from exploitation (Saitov *et al.* 2021; Kopecký and Studer, 2014; Sokolov *et al.*, 2012; Marchenko, Marchenko, and Pedai, 2010; Baker *et al.*, 2007). In this regard, it becomes necessary to develop a sod seeder, which provides lower energy costs and improved working conditions for workers (Lekavičienė *et al.*, 2019). In addition, the development of the seeder is expected to reduce the number of implements needed to create new grass by sowing perennial grass seeds, as well as to increase the efficiency of the process by fertilizing both new and old grass, which will increase profitability, thus contributes to the competitiveness of agriculture (Sysuev *et al.*, 2021; Cheremisinov and Doronin, 2017; Nazarko, 2008). Due to its versatility, the proposed seeder improves direct sowing processes not only for grass seeds but also for grain crops. It also reduces the cost of purchasing various equipment, allowing farmers to receive higher profits. Therefore, the research aims at developing the design of the sod seeder's main working body, i.e. the hoe opener, by conducting theoretical research and obtaining mathematical dependencies to determine the rational parameters and operating modes of the proposed design, which will provide minimal traction force.

2. Methods

An experimental model of an automated sod seeder contains a frame, seed, and fertilizer hopper, seeding units (devices) for seeds and fertilizers, petal agitator, seed and fertilizer pipes, and the main working body – the proposed hoe opener (Figure 1a). The hoe opener consists of (1) a shank, (2) a point attached to the lower part of the shank, (3) a knife, (4) a fertilizers tube; to which (5) a seeds tube is attached at the back side of shank (Kazakhstan Republic, 2021). The lower part of fertilizer tube (4) has a side notch, inside of which a spreader (6) in the form of a cone is installed (Figure 1b).

The shank (1) cuts a vertical slot in the turf with a width of 20 mm, and the knife (3) loosens the soil or turf without turning the layer. The knife horizontally cuts the turf with a width of 100 mm and cuts the roots of old-age grasses, thus avoiding the oppression of the new crop. At the same time, mineral fertilizers are delivered through the fertilizers tube (4) to the conic surface of the spreader (6) and spread evenly in the trace of point (2) and knife (3) at a depth of 8–12 cm. A petal agitator directs seeds into the seeding unit and then the seeds are moved by the seed tube (5) into the soil at the depth of 2–6 cm above the fertilizer layer. The resulting slot is closed (pinched) by the rollers that are mounted on the rear part of the frame.

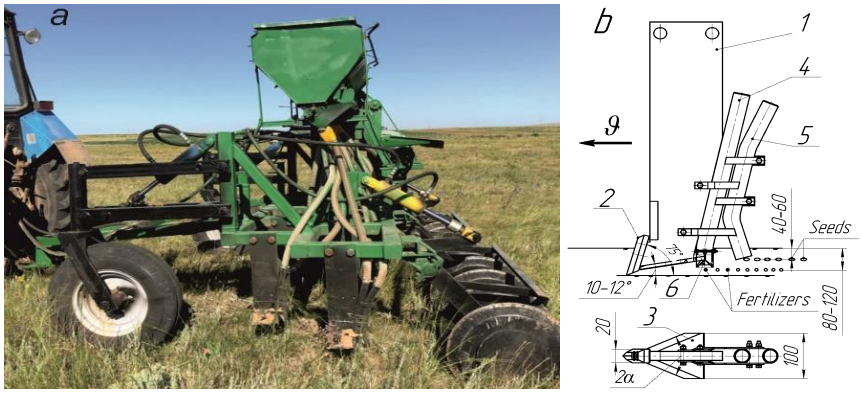

Figure 1 (a) The experimental model of the sod seeder. (b) The design scheme of the experimental hoe opener: 1 – shank; 2 – point; 3 – knife; 4 – fertilizers tube; 5 – seeds tube; 6 – spreader

The seed placement above from the fertilizer horizon excludes their suppression by chemical reactions and contributes to the gradual feeding of the plant root system. The lower, closer to the wet horizon placement of fertilizers promote their better dissolution and migration in the soil environment. Pinching the slots with special rollers prevents the evaporation of moisture through the slots, the withdrawal of the land from the forage turnover, and possible injuries to cattle during grazing. Repeated improvement of the forage area should be made in the perpendicular direction.

Theoretical studies related to the traction force of the new working body are based on the methods of classical mechanics.

To study the influence of the parameters of the hoe opener on its traction characteristics, preliminary laboratory tests on the soil bin were carried out. The soil bin is equipped with a measuring information system and an electronic dynamometer DEP3-1D-10P-2 with data recording on a PC. The maximum permissible relative error is +0.45%.

Field experiments were carried out during the spring and summer periods. The test conditions are shown in Table 1. To determine the tractive forces in the field experiments, this study used a dynamometer (DEP1-1D-50P-2) with the 2nd accuracy class according to ISO 376-2.

Before the field experiments, soil moisture and density were determined. Soil moisture was determined in accordance with GOST 20915-2011 by taking soil samples of field moisture and productive moisture in aluminum boxes by layer horizons in four places located along the diagonal of the plot in 5 cm intervals 0-5, 5-10, 10-15 cm respectively.

Soil density was determined using a soil density meter, i.e., the Wile Soil penetrometer (model 41010). The measurement range was 0 to 3500 kN/m^2. The penetrometer density values show the green segment (0-14 kg/cm^2) (favorable growing conditions), the yellow segment (14-21 kg/cm^2) (acceptable growing conditions), and the red segment (21 kg/cm^2 or more) (an unfavorable growing conditions).

The uniformity of the seed placement depth is determined by direct finding (excavation) of seeds in the row. Seeding units with experimental working tools are determined for each row of working tools (front and rear) by two strips in two adjacent passes of the seeder of one experiment. The indicator of the depth of seeding is the distance from the upper point of the ground cut to the center of the grain. The depth was measured using a ruler with an accuracy of 1 mm.

Table 1 The test conditions

Indicators	Value of indicators
Type of work	Sowing grass seed with simultaneous fertilization
Soil type and name by texture	Southern carbonate chernozem. Heavy loam, turf
Relief	smooth, without slope
Micro-relief	Furrowed
Soil moisture, %, in layers, cm: 0 - 5	16.5
5 - 10	19.46
10-15	21.85
15-20	22.14
20-25	22.65
Soil hardness, MPa, in layers. cm: 0-5	2.1
5-10	**3**.6
10-15	3.5
15-20	3.3
20-25	4.3
Ridgeiness of the field surface, cm	3.2
Pre-treatment	Not treated

3. Results and Discussion

The scheme of forces applied on the hoe opener and its point is shown in Figure 2. The point represents a dihedral angle of *KMM*. Three main elements can be distinguished here: the blade *TKT* (Nukeshev *et al.,* 2023), which is directly involved in soil destruction; chamfers *KM*, KM_1; and frame *M*. The feature of cutting elements of the tillage tool is that the blade at the top *K* of the dihedral angle is quickly worn down and acquires a rounded shape. The chamfers *KM* and KM_1 push aside the material already cut.

Consider the soil particle *A* located on the chamfer of *CM*. Two forces act on it from the side of the chamfer: normal point pressure N_d and friction force F_d. If there is no relative motion of the *A* particle, then after some time it takes position *C*, on the line of translational velocity ϑ. Such behavior of the particle is possible if the friction force between the soil and the point metal F_d and the tangential component of the normal pressure N_{dt} are equal:

$$\mathrm{F}_d = \mathrm{N}_{dt} \quad (1)$$

They are in turn equal to:

$$\mathrm{F}_d = \mathrm{N}_d \cdot tg\varphi$$
$$\mathrm{N}_{dt} = \mathrm{N}_d \cdot ctg\varphi \quad (2)$$

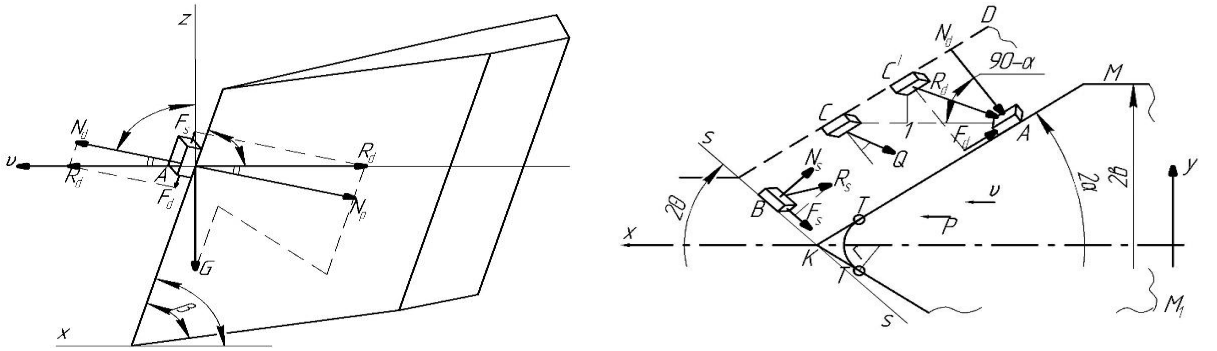

A b

Figure 2 Forces acting on the hoe opener (a) and its point (b). *2α* represents the angle of the hoe opener solution; *2b* represents the width of the working body; *r* denotes the installation angle of the hoe opener; while *β* denotes the installation angle of the working body in the vertical plane

Substituting Equation 2 into Equation 1, we obtain:

$$\varphi = \left(\frac{\pi}{2} - \alpha\right);$$

$$\alpha_{la} = \frac{\pi}{2} - \varphi, \tag{3}$$

here φ is the friction angle between metal and soil; α_{la} is the limit angle of the point blade solution.

Under the condition of Equation 3, the soil particle moves together with the point. For the successful running of the technological process and reducing its energy consumption, the condition must be observed:

$$\alpha_{la} \leq \frac{\pi}{2} - \varphi. \tag{4}$$

At this angle ratio, when the point moves in the soil, particle *A* will not move to point *C*, however, moving in the direction of the resultant force will take the position C_d. In this case, the absolute displacement of the particle is less and equal to the segment AR_d, instead of *AC*, in the absence of sliding. Thus, it is obvious that soil particles undergo complex deformations when the point moves in it – sliding with crumpling. The base of triangle *ARC* fully characterizes the ratio of these deformations. Therefore, segment *A1* characterizes the crumpling deformation of the soil, and segment *C1* characterizes the sliding deformation. Moreover, their ratio can be taken as a measure of deformation in general:

$$\varepsilon = \frac{\mathrm{C1}}{\mathrm{A1}} \tag{5}$$

Using the sine theorem from triangle *ACC′* we have:

$$\mathrm{C1} = \mathrm{C'1}\frac{\cos\alpha}{\sin\alpha};$$

$$A1 = C'1\frac{sin(\alpha+\varphi)}{cos(\alpha+\varphi)};$$

$$\xi = \frac{ctg\alpha}{tg(\alpha+\varphi)}. \tag{6}$$

$$\xi = \frac{1}{tg\alpha \cdot tg(\alpha+\varphi)}.$$

It can be seen from Equation 6 that the measure of soil deformation with a point depends on two values: the angles of the point blade solution and external friction. Moreover, this dependence is inversely proportional; as the solution angle increases, the slip decreases, and the deformation of the crumple increases. On the rectilinear section of the *TM* chamfer, the nature of soil deformation does not change. The ratio of slip measures *C1* to crumpling measures *A1* is constant or closer to constant. However, it is violated on

the curvilinear section *T–T*. In the center of the arc, the directions of translational velocity ϑ and normal pressure P_d coincide. In this case, a slip does not occur, and the clean crumpling of the soil originated.

The sliding of the particle will begin after the *T* point, and the crumpling of the soil is on the wane. Their (*C1* and *A1*) ratios will be established. The maximum savings in energy costs will occur when the soil is treated with a clean slip. Such a case may occur at $\alpha \to 0$, and it is unrealistic since in this case soil loosening will not occur. Therefore, such soil processing is unproductive. It can be assumed that the determining position will be such that the measures of crumpling and sliding will be equal or the first will be somewhat less than the second. At the same time, energy consumption will be minimal, and the soil will receive treatment. In this case:

$$C1 \leq A1$$

This condition will be fulfilled if the triangle ACC' is isosceles. In this case, the angles:

$$\angle C'CA = \angle C'AC$$

where:

$$\angle C'CA = \alpha$$

$$\angle C'AC = \left(\frac{\pi}{2} - \alpha\right) - \varphi.$$

From the last three equations we obtain:

$$\alpha = \frac{\pi}{4} - \frac{\varphi}{2}.$$

Obviously, for the sliding to be greater than the crumpling, it is necessary to:

$$\alpha \geq \frac{\pi}{4} - \frac{\varphi}{2}. \quad (7)$$

Thus, Equation 4 and Equation 7 give the condition for choosing the angle of solution of the tillage tool, i.e., the point, and its lower and upper limits, which will ensure tillage with sliding and crumpling:

$$\frac{\pi}{4} - \frac{\varphi}{2} \leq \alpha \leq \frac{\pi}{2} - \varphi \quad (8)$$

To justify the angle of installation of the working body in the vertical plane, consider Figure 2a. The pushing force of the working body R_d acts on particle *A*. It can be separated into the normal N_d and tangential components F_d. In this case, the angle between the normal and resultant forces is equal to φ, and the angle between the normal and the vertical axis is equal to β. The external, pushing force is counteracted by the gravitational force *G* and the internal ground adhesion force F_s and the frictional force *F*. The latter force can be accounted for by the coefficient of internal friction. According to the 3rd law of mechanics, the external forces R_d and N_d are counteracted by R_p and N_p equilibriums.

Consider equilibrium effects of active forces on natural axis – in the direction of point chamfer.

$$-F_д + F_s - Gsin\beta = 0; \quad (9)$$

$$N = Gcos\beta.$$

Here the weight of the soil element $G = mg$, and the frictional forces differ by the internal and external coefficients f_1 and *f*, respectively, where:

$$-fmgcos\beta + f_1 mgcos\beta = mgsin\beta$$

$$(f_1 - f) = tg\beta; \quad (10)$$

The values of the coefficients are $f_1 = 0.84$; $f = 0.58$. In this case $\angle\beta = 15°$, *m* denotes the mass of the cultivated soil element; and *g* represents the acceleration of gravity. With this setup, the hoe opener will not work satisfactorily, since the point works to lift the soil layer, not to cut it. Undeformed clods will create slumping furrows.

The hoe opener will work steadily if its thrust force is directed horizontally or closer to it. Therefore, it is important to consider the equilibrium of active forces in the direction of the horizontal axis:

$$F - F_s \cdot cos\beta - Ncos\varphi = 0 \quad (11)$$

Substituting the values of the components in Equation 11, we obtain:

$$cos\varphi = (f_1 - f)cos\beta, \quad (12)$$

where from:

$$cos\beta = \frac{cos\varphi}{(f_1 - f)}. \quad (13)$$

Using the above values and taking into account that $f = tg\varphi$ we obtain:

$$cos\beta = \frac{0.86}{0.26} = 3.3; \quad \beta = 73°$$

The resulting angle is quite satisfactory. The point in the turf cuts slots with the required size, where seeds and fertilizers are applied.

To determine the traction force of the hoe opener, consider the equilibrium of external forces acting on it in the directions of the horizontal and vertical axes:

$$R_s sin(\theta + \varphi_1) + Qsin(\alpha + \varphi_1) + R_d sin(\alpha + \varphi) = P; \quad (14)$$

$$R_s cos(\theta + \varphi_1) - Qcos(\alpha + \varphi_1) - R_d cos(\alpha + \varphi) = 0, \quad (15)$$

Where: R_s denotes the shear resistance force on the shear plane *LK*; *Q* denotes the force of inertia of soil elements arising during its movement; R_d denotes the resistance force of soil elements to compression deformation by the point; *P* denotes the force applied to the working body; φ_1 denotes the angle of soil internal friction; and θ denotes the angle of soil shear. From Equation 15 we define:

$$R_d = R_s \frac{cos(\theta+\varphi_1)}{cos(\alpha+\varphi_1)} - Q \frac{cos(\alpha+\varphi_1)}{cos(\alpha+\varphi)}. \quad (16)$$

Substituting the Equation 16 into the Equation 15:

$$P = R_s \left[sin(\theta + \varphi_1) + \frac{cos(\theta + \varphi_1) \cdot sin(\alpha + \varphi)}{cos(\alpha + \varphi_1)} \right] + \\ + Q[sin(\alpha + \varphi_1) - cos(\alpha + \varphi_1) \cdot tg(\alpha + \varphi)] \quad (17)$$

The last equation is presented in a simplified form:

$$P = R_s(\mathrm{A} + \mathrm{B}_1) + Q(\mathrm{A} - \mathrm{B}_2) \quad (18)$$

where: $\mathrm{A} = \sin(\theta + \varphi_1)$; $B_1 = \frac{\cos(\theta+\varphi_1)\cdot\sin(\alpha+\varphi)}{cos(\alpha+\varphi_1)}$; $B_2 = cos(\alpha + \varphi_1) \cdot tg(\alpha + \varphi)$.

It can be seen from Equation 17 that the traction force of the hoe opener is composed of two independent quantities: the first is the resistance of the soil to shear deformation, and the second is the resistance of the soil elements to the acquisition of kinetic energy, that is, movement, which in turn depend on the solution angle, installation angle of the working body, and the external and internal friction angles of the soil.

The reaction of the undeformed formation in front of the point is formed by the shear resistance, which is equal to the:

$$R_z = 2LK \cdot h \cdot \sigma_{ur}\,, \quad (19)$$

where:

$$LK = \frac{b}{sin\theta}.$$

herewith:

$$R_z = \frac{2bh}{sin\theta}\sigma_{ur}\,. \quad (20)$$

here: *h* denotes the working body stroke depth; σ_{ur} denotes the ultimate resistance of the soil to compression; and ρ denotes the volumetric weight of the soil.

According to Newton's Law 2, the displaced elements of the soil acquire the force of inertia:

$$Q = \omega m, \tag{21}$$

where: ω denotes the acceleration of moving elements; m denotes the mass of moving elements.

The acceleration of the movable element ω (Equation 21) is equal to:

$$\omega = \frac{\vartheta_a - \vartheta_0}{t - t_0} = \frac{\vartheta_a}{t} \quad , \tag{22}$$

where: initial velocity $\vartheta_0 = 0$ and initial time $t_0 = 0$; ϑ_α denotes the absolute velocity of the soil element; and t denotes the travel time of the element on the chamfer.

The travel time on the *KM* chamfer is equal to:

$$t = \frac{\text{KM}}{\vartheta_0} = \frac{b}{2\vartheta_0 sin\alpha}. \tag{23}$$

To determine the velocities of the soil element, consider the velocity plan in Figure 3:

$$\angle 312 = \frac{\pi}{2} - \alpha;$$

$$\angle 412 = \frac{\pi}{2} - (\alpha + \varphi);$$

$$\angle 241 = \frac{\pi}{2} + \varphi.$$

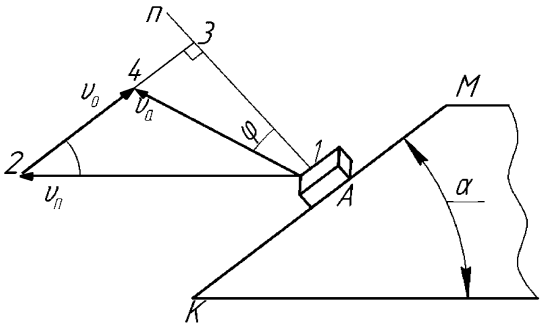

Figure 3 Velocities of moving soil elements

herewith:

$$\vartheta_a = \vartheta \frac{sin\alpha}{\varphi};$$

$$\vartheta_0 = \vartheta \frac{cos(\alpha+\varphi)}{cos\varphi} \quad . \tag{24}$$

Substituting Equations 23 and 24 in Equation 22 we define:

$$\omega = \vartheta^2 \frac{sin\alpha}{cos(\alpha+\varphi)} \quad . \tag{25}$$

In Equation 21 the mass of the deformable soil layer is determined:

$$m = KM \cdot KL \cdot h \cdot g\,,$$

where:

$$KM = \frac{2b}{sin\alpha};\ \ KL = \frac{2b}{sin\theta}$$

$$m = \frac{b^2 h \cdot \rho \cdot 4}{sin\alpha \cdot sin\beta}. \tag{26}$$

Taking into account Equations 25, 26 and 21 take the form:

$$Q = \vartheta^2 \frac{h \cdot \rho \cdot b^2 \cdot 4}{sin\beta \cdot cos(\alpha+\varphi)}. \tag{27}$$

Substituting Equation 20 and Equation 27 in Equation 18 obtain:

$$P = \frac{2bh\sigma_{ur}}{sin\theta}(A + B_1) + \vartheta^2 \frac{h \cdot \rho \cdot b^2 \cdot 4}{sin\beta \cdot cos(\alpha+\varphi)}(A - B_2). \tag{28}$$

From the equation of the traction force of the hoe opener (Equation 28), we can see that the first term is resistance averaged from the parameters of the tilled soil layer and its physical and mechanical characteristics, such as shear deformation angle and ultimate compression resistance, and the second term is inertial resistance to movement of soil

elements, depending on the translational velocity of the tool and its installation, solution, and friction angles.

In order to verification of calculations and results, the average numerical values of the variables included in the obtained formulas have been taken based on known theoretical data (Panov and Vetokhin, 2008; Sineokov and Panov, 1977), they are: α = 30°; φ = 30°; φ_1 = 40°; θ = 45°; β = 75°; $2b$ = 0.03 m; h = 0.1 m; ϑ = 2.77 m/s; σ_{ur} = 15 kg/cm; $\rho = 10^3$ kg/cm. Accordingly, they obtain: A = 0.087; B_1 = 0.22; B_2 = 592; R_z = 748.93 N; Q = 28.19 N. The traction force of the working body is equal to P = 720.73 N. The obtained result is close to the expected one. A comparison with other simulation studies (Afify *et al.*, 2020) shows that the findings are significantly lower than the traction forces of the models investigated by other researchers, especially when with a dependence on tool rake angle and tool depth.
Approximation of the experimental data (Figure 4) of the dependence of the experimental colter traction resistance on the velocity of translational motion allowed us to obtain the following equations:
at the minimum velocity:

$$y = 123.57x^2 - 59.893x + 243.14$$

$$R^2 = 0.9081$$

at the average velocity:

$$y = 47.857x^2 - 56.393x + 520.44$$

$$R^2 = 0.977$$

at the maximum velocity:

$$y = 17.143x^2 - 54.857x + 851.8$$

$$R^2 = 0.8758.$$

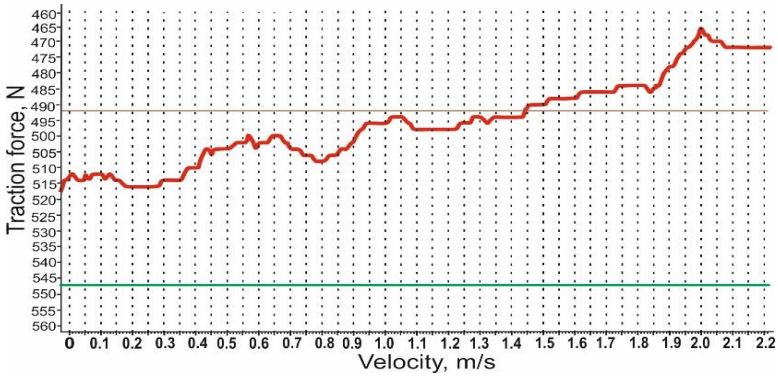

Figure 4 The graph of traction force obtained by the electronic dynamometer (at average velocity)

According to the results obtained by the dynamometric method, the force of one tool at a working depth of 0.1 m varied from 238 to 808 N at speeds of 0.1–1.75 m/s. Change of traction force depending on motion velocity has a parabolic character. This is explained by the fact that at the initial moment of the interaction of the working body with the soil, the inertial forces arise because at this time the resting inertia of the soil is violated, its particles acquire certain accelerations and a certain absolute velocity, which does not coincide with the motion (sliding) line. The inertial force will be directed along the line of the absolute velocity of the particles, only in the opposite direction. In the steady-state process of soil disintegration, the tractive force is minimal. However, as the translational velocity increases further, the tractive force also increases. Determination of the total traction force of the experimental sod seeder under field conditions showed that it varies from 8.28 to 8.63 kN. The decrease of traction force on the experimental seeder is explained by the

decrease in the length of the point working surface and the change of its installation angle up to 75° relative to the horizon.

Experiments have shown that the velocity of the unit has a significant influence on the value of traction resistance of the seeder with experimental working tools. With an increase of velocity from 3.7 to 8 km/h, the traction resistance of the experimental seeder sample increases by 4–4.5%, and it is lower than indicators of the prototype (Eurasian Patent, 2021) by 0.11–0.15 kN (Figure 5).

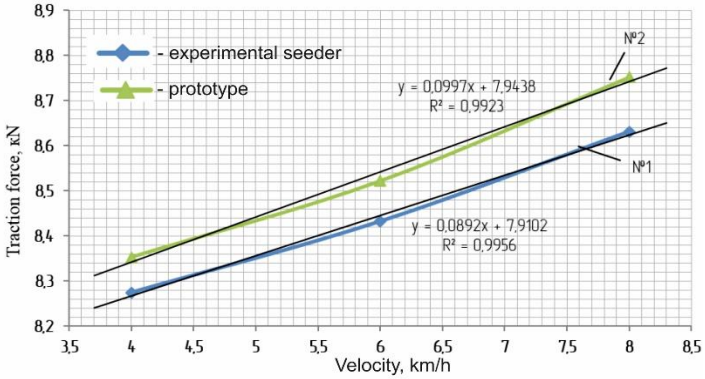

Figure 5 Dependence of tractive force on the velocity of the units

Field experiments with seeding grass seeds into the turf have demonstrated that the experimental model of the seeder provides a stable technological process of seeding hard-to-bulk grass seeds at the depth of 1.8–6 cm with a simultaneous site-specific application of mineral fertilizers at the depth of 8–12 cm. The surface of the field after the passage of the seeder is characterized by an even turf relief with traces (20 mm wide) of the working body shank. Visual observation of the hoe opener operation at low speeds showed that the knife (Figure 1a) loosens the soil or turf without turning the layer. At the same time, it cuts the roots of old-age grasses and promotes the formation of soil interlayer between fertilizer and seeds. Installation of the point at an angle of 75° to the horizon excludes a soil layer turnover.

The results of the laboratory and field tests allowed us to determine the technical characteristics of the experimental planter (Table 2).

Table 2 Technical characteristics of the sod seeder

Indicators	Meanings
Type of aggregation	Trailerized
Aggregate class,	1-3
Working speed, km/hour max.	7.6-10
Working width, m	3,6
Row spacing, cm	35
The number of rows to be tilled at the same time, pcs.	11
Productivity, ha/h	2.5-3.0
Depth of sowing of grain crops, cm	2-8
Depth of grass seed placement, cm	1.8-6
Fertilizer placement depth, cm	8-12
Overall dimensions of a planter in the transport position, mm, max:	
- Length, mm	4000
- width, mm	3500
- height, mm	2100
Weight (dry), kg	2500
Ground clearance, mm not less	300
Traction force, kN	8.28-8.63

Further research will be aimed at improving the colter to ensure uniform application of liquid complex fertilizers during sowing under cover crops and in the turf.

4. Conclusions

Based on theoretical studies, substantiated that the traction force (759 N), as well as the solution (25°–45°) and installation (73°–76°) angles of the hoe opener, depend on its constructive and technological parameters. Determination of the total traction force of the experimental sod seeder in field conditions has shown that it varies within the range 8.28–8.63 kN by increasing the velocity from 3.7 to 8 km/h and the traction resistance of the experimental sample of seeder grows on 4–4.5%, thus it is lower than indicators of the prototype sample on 0.11–0.15 kN. Field experiments where performed grass seeds seeding into the turf have shown that the experimental model of the sod seeder provides a stable technological process of seeding hard-to-bulk grass seeds at the depth of 1.8–6 cm with a simultaneous site-specific application of mineral fertilizers at the depth of 8–12 cm. The surface of the field after the passage of the sod seeder is characterized by an even turf relief with traces (20 mm wide) of the working body's shanks and knife. Visual observation of the work of a new working body at low speed showed that the knife loosens the soil or turf without turning the soil layer and at the same time it cuts roots of old-age grasses thereby promoting the formation of a soil layer between fertilizer and seeds. Installation of the point at an angle of 75° to the horizon eliminates the turn of the soil layer.

Acknowledgments

This research was funded by the Ministry of Education and Science of the Republic of Kazakhstan, grant number AP05134800 (2018-2020) titled 'The development of automated grain-fertilizer-grass seeder for site-specific direct sowing of agricultural crops under cover crops and sod with simultaneous application of mineral fertilizers'.

References

Adams, J., Samimi, C., Mitterer, C., Bendix, J., Beck, E., 2022. Comparison of Pasture Types in The Tropical Andes: Species Composition, Distribution, Nutritive Value and Responses To Environmental Change. *Basic and Applied Ecology,* Volume 59, pp. 139–150

Afify, M. T., EL-Haddad, Z.A., Lamia, A.A.D., 2020. Modeling The Effect of Soil-Tool Interaction on Draft Force Using Visual Basic. *Annals of Agricultural Science, Moshtohor,* Volume 58(2), pp. 223–232

Baker, C.J., Saxton, K.E., Ritchie, W.R., Chamen, W.C.T., Reicosky, D.C., Ribeiro, M.F.S., Justice S.E., Hobbs P.R., 2007. *No-tillage Seeding in Conservation Agriculture.* 2nd Edition. FAO and CAB International. UK: Cromwell Press, Trowbridge

Bathgate, A., Revell, C., Kingwell, R., 2009. Identifying The Value of Pasture Improvement Using Wholefarm Modelling. Agricultural Systems, Volume 102(1–3), pp. 48–57

Benincasa, P., Zorzi, A., Panella, F., Tosti, G., Trevini, M., 2017. Strip Tillage and Sowing: Is Precision Planting Indispensable in Silage Maize? *International Journal of Plant Production,* Volume 11(4), pp. 577–588

Bowman, M.T., Beck, P.A., Watkins, K.B., Anders, M. M., Gadberry, M. S., Lusby, K. S., Gunter, S. A., Hubbell, D. S., 2008. Tillage Systems for Production of Small-Grain Pasture. *Agronomy journal,* Volume 100(5), pp. 1289–1295

Cheremisinov, D.A., Doronin, M.S., 2017. On The Development of The Technological Scheme of a Seeder for Seeding Grass Seeds Into Turf. *In*: Mat. III International Scientific and

Practical Conference Methods and Technologies in Plant Breeding and Crop Production, pp. 406–410

Deák, B., Becker, T., Boch, S., Wagner, V., 2018. Conservation, Management and Restoration of Semi-Natural and Natural Grasslands in Central Europe - Editorial To The 13th EDGG Special Feature. *Tuexenia,* Volume 38, pp. 305–310

Eurasian Patent, 2021. Eurasian Patent No. 038584. Grain Fertilizer-Grass Anti-Erosion Seeder / KATU Named After S. Seifullin

Fulkerson, W.J., Lowe, K.F., 2022. Perennial Forage and Pasture Crops - Establishment snd Maintenance. *Encyclopedia of Dairy Sciences*. 3rd Edition. Academic Press. pp. 759–768

Himmelbauer, M.L., Vateva, V., Lozanova, L., Loiskandl, W., Rousseva, S., 2013. Site Effects on Root Characteristics and Soil Protection Capability of Two Cover Crops Grown in South Bulgaria. *Journal of Hydrology and Hydromechanics,* Volume 61(1), pp. 30–38

Karimipoor, Z., Rashtian, A., Amirkhani, M., Ghasemi, S., 2021. The Effect of Grazing Intensity on Vegetation Coverage and Nitrogen Mineralization Kinetics of Steppe Rangelands of Iran (Case Study: Nodoushan Rangelands, Yazd, Iran). *Sustainability*, Volume 13 (15), p. 8392

Kazakhstan Republic, 2021. Kazakhstan Republic Patent No. 35155, Cereal Seeder (№2020/0206.1) / KATU Named After S.Seifullin

Kopecký, D., Studer, B., 2014. Emerging Technologies Advancing Forage and Turf Grass Genomics. *Biotechnology Advances,* Volume 32(1), pp. 190–199

Lekavičienė, K., Šarauskis, E., Naujokienė, V., Buragienė, S., Kriaučiūnienė, Z. 2019. The Effect of The Strip Tillage Machine Parameters on The Traction Force, Diesel Consumption and CO2 Emissions. *Soil and Tillage Research*, Volume 192, pp. 95–102

Marchenko, O.S., Marchenko, N.M., Pedai, N.P., 2010. Combined Aggregate MPTD-12 for Strip Sowing of Grass Seeds and Grass Mixtures on Meadows and Pastures. *Agricultural Machinery and Technology*, Volume 5, pp. 15–17

Nazarko, O., 2008*. Seeding Forages into Existing Shanks Using Minimal Tillage*. Report Manitoba Forage Council 06.08, Canada's Agricultural Producers Addressing Environmental Issues (CAPAEI) Program, Winnipeg, Canada

Nukeshev, S., Yeskhozhin, K., Karaivanov, D., Ramaniuk, M., Akhmetov, E., Saktaganov, B., Tanbayev, K., 2023. A Chisel Fertilizer for In-Soil Tree-Layer Differential Application in Precision Farming. *International Journal of Technology*, Volume 14(1), pp. 109–118

Panov, I.M., Vetokhin, V.I., 2008. Physical Bases of Soil Mechanics. Ukraine: Phoenix

Revenko, V.YU., Belousov, M.M., 2014. Test Results of a Machine for Strip-Seeding Grass in Turf. *International Agroengineering,* Volume 4(12), pp. 53–61

Saitov, V., Kurbanov, R., Demshin, S., Sozontov, A., 2021. Improving of the sod seeders SDK of strip grass seed sowing. *In*: Mottaeva, A. (eds) Proceedings of the XIII International Scientific Conference on Architecture and Construction 2020, Volume 130

Scotton, M., 2019. Mountain Grassland Restoration: Effects of Sowing Rate, Climate and Soil on Plant Density and Cover. *Science of the Total Environment,* Volume 651, pp. 3090–3098

Sineokov, G.N., Panov, I.M., 1977. Teoriya i Raschet Pochvoobrabatyvayushchih Mashin (*Theory and Calculation of Tillage Machines*). Russia: Mashinostroenie

Sokolov, A.V., Zamana, S.P., Patlai V.V., Fedorovsky T.G., Kindsfater, V.Y., 2012. Improving The Technological Process and Means for Direct Grasses Undersowing into Grassland Sod of Natural Fodder Lands. *Fodder Production,* Volume. 4, pp. 44–46

Soldatov, E., Dzhibilov, S., Soldatova, I., Guluyeva, L., 2020. Restoration of Degraded Mountain Pastures of The Central Caucasus by Targeted Sowing of Seeds of Perennial Grasses. *In*: E3S Web of Conferences, Volume 175

Sysuev, V., Kurbanov, R., Demshin, S.L., Saitov, V.E., Doronin, M.S., 2021. Parameters and Operating Modes of The Coulter Group of The Sod Seeder. *In*: IOP Conference Series: Earth and Environmental Science, Volume 723, p. 022050

Sysuev, V.A., Demshin S.L., Gaididei S.V., 2022. Results of Research of The Combined Seeder for Strip Sowing of Grasses Into Sod. *Agricultural Science Euro-North-East*, Volume 23(2), pp. 263–273

Zhao, T., Zhao, Y., Higashi, T., Komatsuzaki, M., 2012. Power Consumption of No-Tillage Seeder Under Different Cover Crop Species and Termination for Soybean Production. Engineering in Agriculture. *Environment and Food*, Volume 5(2), pp. 50–56,

Zotov, A.A., Kosolapov, V.M., Kobzin, A.G., Trofimov, I.A., Ulanov, A.N., Shevtsov, A.V., Shel'menkina Kh., Shchukin, N.N., 2012. Senokosy I Pastbishcha Na Osushaemykh Zemlyakh Nechernozem'ya (*Hayfields and Pastures on The Drained Lands of The Non-Chernozem Region*). Kazkhstan: IP Izotova K.U.